Electronic Supplementary Material (ESI) for Chemical Communications

Electronic Supporting Information (ESI) concerning the manuscript:

Photomagnetic effect in a cyanide-bridged mixed-valence $\{Fe^{II}_2Fe^{III}_2\}$ molecular square

Abhishake Mondal, Yanling Li, Patrick Herson, Mannan Seuleiman, Marie-Laure Boillot, Eric Rivière, Miguel Julve, Lionel Rechignat, Azzedine Bousseksou, and Rodrigue Lescouëzec

Experimental Section

Syntheses. The bik ligand and the $PPh_4[Fe^{III}(Tp)(CN)_3]\cdot H_2O$ complex were prepared as previously described.[S1] The air stable $[Fe(bik)_2(S)_2]Cl_2$ complex was prepared *in situ* by reaction of stoichiometric amounts of $FeCl_2\cdot 4H_2O$ and bik in methanol. The methanolic solution of $PPh_4[Fe^{III}(Tp)(CN)_3]\cdot H_2O$ was added dropwise to that containing $[Fe(bik)_2(S)_2]Cl_2$. The resulting bluish-red solution was stirred at room temperature for 30 min and then filtered. Slow evaporation of the filtrate under ambient conditions afforded orange-red plate-like crystal of $\{[Fe^{III}(Tp)(\mu\text{-}CN)_2(CN)]_2[Fe^{II}(bik)_2]_2\}$ $[Fe^{III}(Tp)(CN)_3]_2\cdot 18H_2O\cdot 4CH_3OH$ in few days. Elemental analyses match with partially dehydrated sample of formula: $\mathbf{1}\cdot 6H_2O\cdot 2CH_3OH$ calcd (%) for $C_{86}H_{100}B_4Fe_6N_{52}O_{12}$: C 42.47, H 4.14, N 29.94; found: C 42.03, H 3.58, N 29.85; FT-IR (KBr, 300 K, fresh sample): ν = 2514 cm^{-1} (ν_{BH}), 2123, 2147 and 2160 cm^{-1} (ν_{CN}) and 1630 cm^{-1} ($\nu_{C=O}$).

S1. (a) N. Braussaud, T. Ruther, K. J. Cavell, B. W. Sketon and A. H. White, *Synthesis*, 2001, 626; (b) R. Lescouëzec, J. Vaissermann, F. Lloret, M. Julve, M. Verdaguer, *Inorg. Chem.,* 2002, **41**, 5943.

Physical Techniques.

Elemental Analysis (C, H, N) were carried out at the SIARE service of the Université Pierre et Marie Curie, Paris6.

Thermogravimetric analysis has been carried out on a TAI instrument SDT Q600 under 1 bar dinitrogen atmosphere.

FT-IR spectra were collected in the 200-4000 cm^{-1} range. Room temperature measurements were carried out on a Tensor 27 Bruker instrument working in the ATR mode, while variable-temperature studies (between 108 and 313 K) were performed on a Perkin Elmer spectrometer (Spectrum 100) equipped with the eurolabo variable-temperature cell (21525) and Specac temperature controller (20120). The FT-IR measurement of the dehydrated phase has been recorded immediately after the TGA experiment (the FT-IR spectrum did not change when leaving the sample in air).

Variable-temperature solid-state UV-Vis spectra were measured in the range 350-2500 nm on a CARY 5000 double-beam spectrophotometer equipped with an APD Cryogenic closed-cycle helium system including a DMX-1E cryostat and a DE-202 expander.

Variable-temperature (2-400 K) magnetic measurements were carried out with a Quantum Design SQUID magnetometer. In a typical experiment, a fresh sample was introduced at 200 K under helium flow and frozen before purging under vacuum. The measurements are carried out from 200 K to 2 K first and then from 2 K to higher temperatures. Dehydrated samples have been prepared and measured immediately after TGA experiments.

Mössbauer Spectroscopy. ^{57}Fe Mössbauer spectra have been recorded using a conventional constant-acceleration-type spectrometer equipped with a 50 mCi ^{57}Co source and a flow-type, liquid-helium cryostat. Spectra of the samples (ca. 50 mg) were recorded between 300 and 80 K. Least-squares fittings of the Mössbauer spectra have been carried out with the assumption of Lorentzian line shapes using Recoil software package.

Crystal Structure Data Collection and Refinement. Crystal data for **1**$\cdot 18H_2O \cdot 4CH_3OH$: $C_{88}H_{132}B_4Fe_6N_{52}O_{26}$, $M_r = 2712.68$ g$\cdot$mol^{-1}. Data were collected at 200(2) K on a Bruker APEX-II CCD diffractometer with graphite mono-chromated Mo-Kα radiation ($\lambda = 0.71073$ Å) and the ω and Φ scan. Data were corrected for Lorentz and polarization effects, and an semi-empirical absorption correction based on symmetry equivalent reflections was applied by using the SADABS program [G.M. Sheldrick, SADABS, Program for Scaling and Correction of Area Detector Data, University of Göttingen, Göttingen (Germany) 1997, R.H. Blessing, *Acta Cryst A*, 1995, **33**, 51]. Lattice parameters were obtained from least-squares analysis of 9924 reflections, $3 < \theta < 30°$, triclinic, space group *P-1*; cell parameters: a = 13.1932(4) Å, b = 13.2686(4) Å, c = 20.6938(8) Å, α = 96.856(2)°, β = 107.338(1)°, γ = 113.861(1)°, V = 3138.52(19) Å^3 and Z = 1.The structure was solved by direct methods using SHELXS86(Sheldrick, G.M. (1986). SHELXS86. Program for the solution of crystal structures. Univ. of Gottingen, Germany), and refined with full-matrix least-squares technique on F^2 using the CRYSTALS programs Watkin, D.J., Prout, C.K., Carruthers, J.R., Betteridge, P.W. & Cooper R.I. (2001) CRYSTALS Issue 11. Chemical Crystallography Laboratory, OXFORD, UK). All non-hydrogen atoms (except those of the solvent molecules) were refined anisotropically. All hydrogen atoms were set on calculated positions and isotropically refined. Refinement gave $R1[I > 2\sigma(I)]$ / R_{w2} 0.063 / 0.195 (for all data); max/min residual electron density: 1.56 / –1.12 e Å^{-3}. The goodness-of-fit is 0.961.

Figure S1. View of the hydrogen bond pattern interlinking the $\{Fe^{III}_2Fe^{II}_2\}$ square unit and the paramagnetic $[Fe^{III}(Tp)(CN)_3]^-$ counterions through the water molecules in **1.**

Figure S2. Thermo-gravimetric analysis of **1** in the 20-400 °C range at 1°C/min (under a dinitrogen atmosphere).

Figure S3. Variable-temperature FT-IR spectra of the dehydrated phase of **1** in the ranges 400-2000 (top) and 2000-2200 cm^{-1} (bottom).

Figure S4. Magnetization *vs*. irradiation time of a dehydrated sample of **1** at different wavelengths (7 mW/cm^2).

Figure S5. Solid-state UV-Vis absorption spectra of **1** at different temperatures (sample diluted in a KBr pellet).

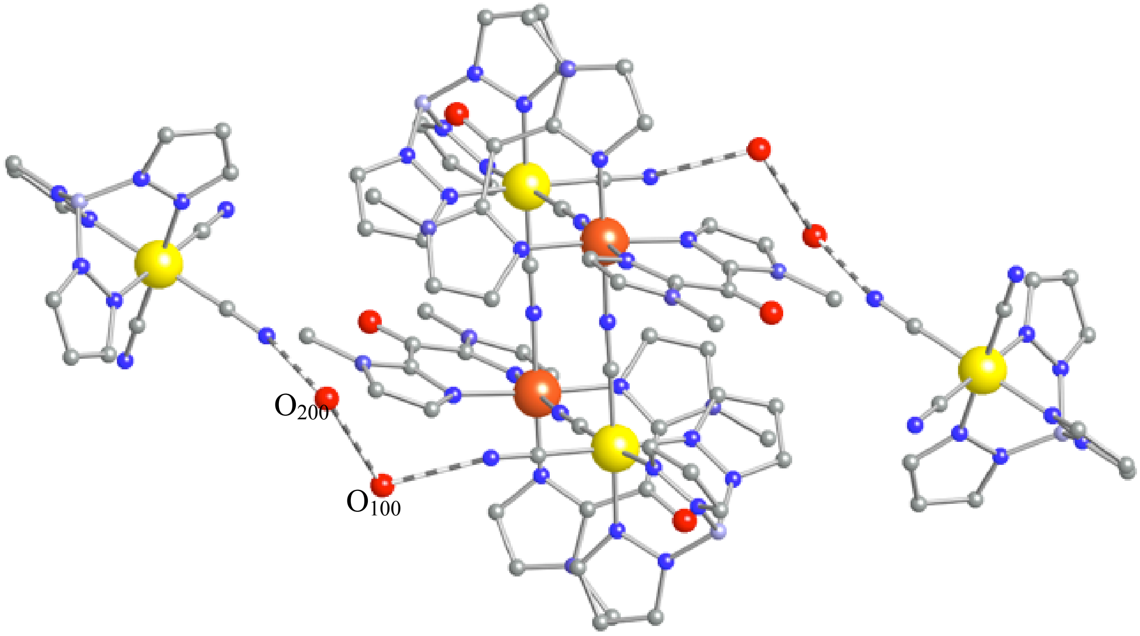

Figure S1. View of the hydrogen bond pattern interlinking the $\{Fe^{III}{}_2Fe^{II}{}_2\}$ square unit and the paramagnetic $[Fe^{III}(Tp)(CN)_3]^-$ counterions through the water molecules in **1.**

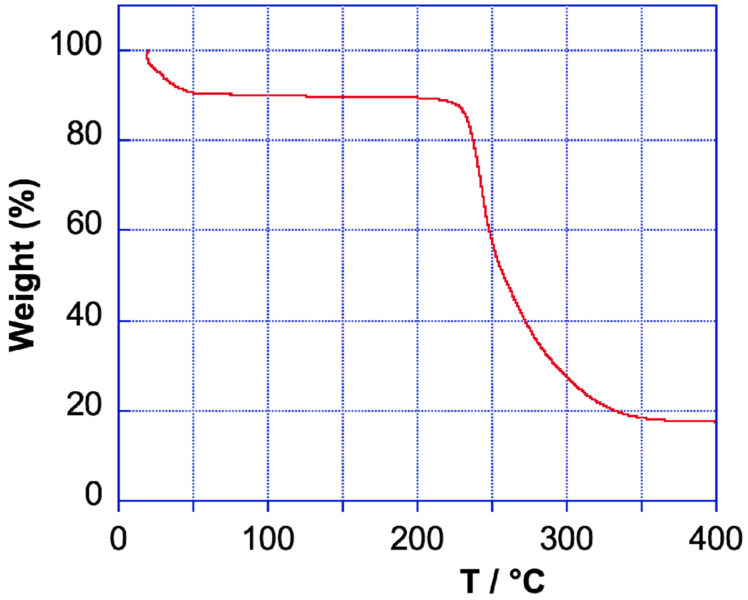

Figure S2. Thermo-gravimetric analysis of **1** in the 20-400 °C range at 1°C/min (under a dinitrogen atmosphere).

Compound **1** has been studied by thermogravimetric analysis (TGA). It exhibits a significant weight loss from room temperature up to 50 °C, which corresponds to about 11% of the total sample mass. At higher temperatures, the compound seems to be stable under dinitrogen atmosphere up to ca 200 °C. The important weight loss observed at room temperature is smaller than the expected value (16%) for a total release of the solvent molecules, but it is consistent with the rapid loss of crystallinity of **1** as the sample is removed from the mother liquor. Most likely, the sample has already lost some solvent molecules before launching the TGA measurements.

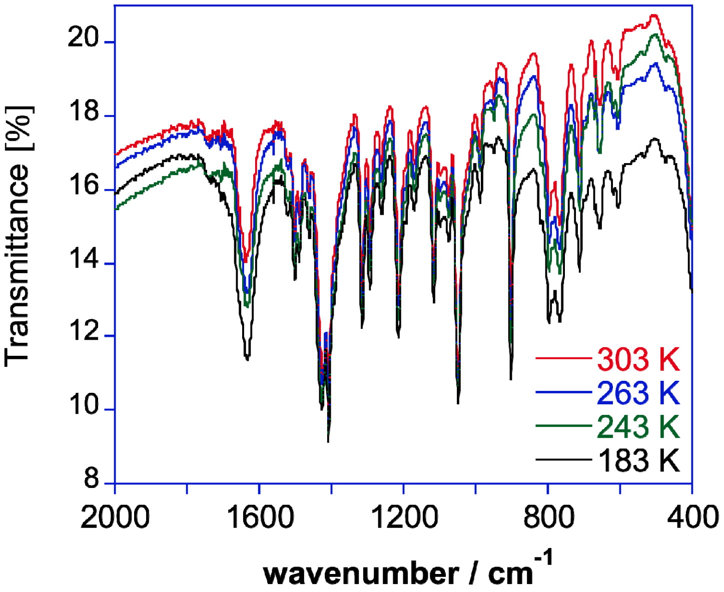

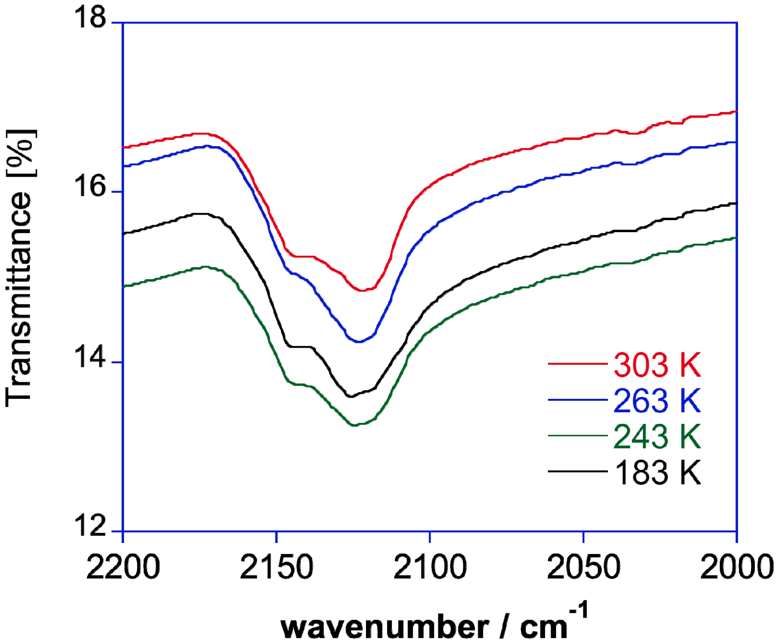

Figure S3. Variable temperature FT-IR spectra of the dehydrated phase of **1** in the ranges 400-2000 (top) and 2000-2200 cm^{-1} (bottom).

The FT-IR spectra of the dehydrated phase of **1** exhibit only slight shifts of the cyanide stretching frequencies around the thermo-induced spin transition ($T_{1/2}$ = 240 K). In particular, no peaks are observed below 2100 cm^{-1} excluding the occurrence of the Fe^{II}_{LS}-CN unit. Overall these small shifts do not match with an electronic transfer in the Fe^{III}_{LS}-CN-Fe^{II}_{LS} pair but they are more consistent with a thermo-induced mechanism centred on the Fe^{II} ion.

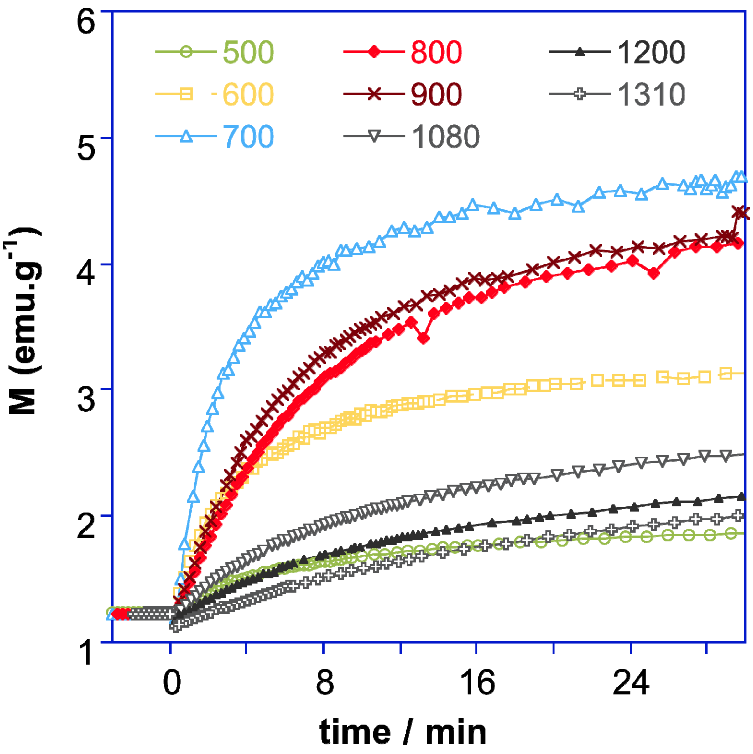

Figure S4. Magnetization *vs.* irradiation time of a dehydrated sample of **1** at different wavelengths (7 mW/cm^2).

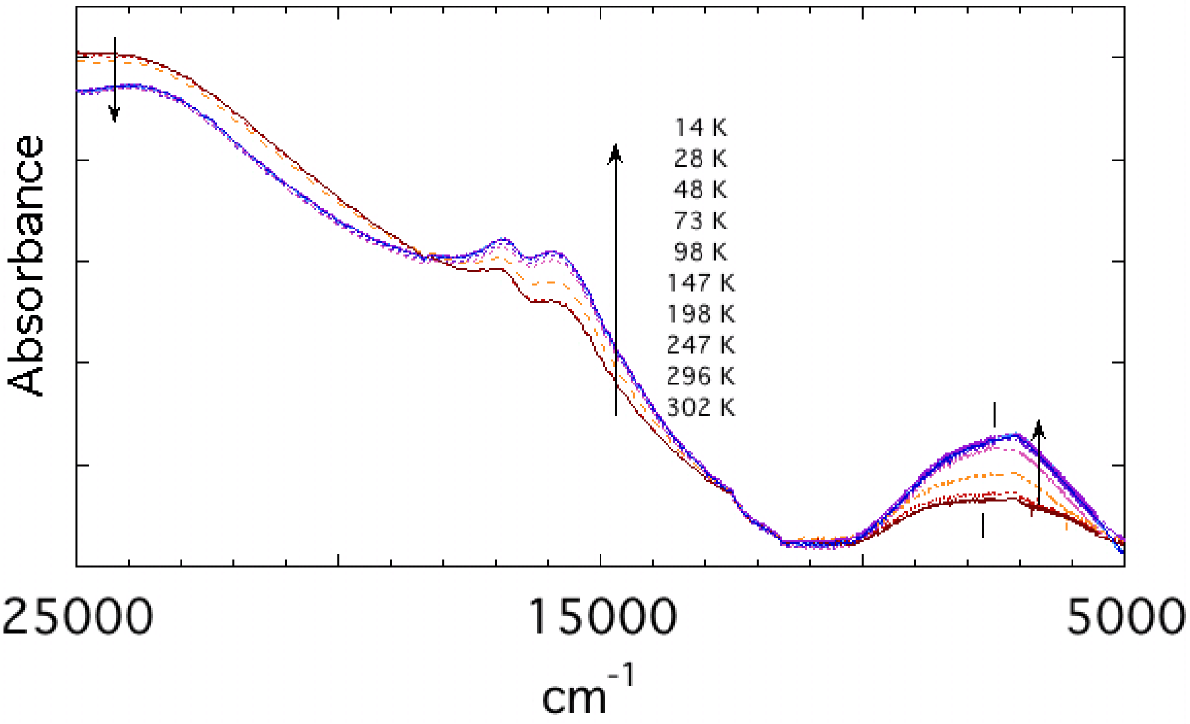

Figure S5. Solid-state UV-Vis absorption spectra of **1** at different temperatures of a sample diluted in a KBr pellet.

The bands located near 16000 cm^{-1} (or 625 nm) can be ascribed to metal-to-ligand charge transfer (MLCT) in the iron(II) chromophore while that centred at 7200 cm^{-1} in the near-IR can be ascribed to intervalence charge transfer (IVCT).